Nanoscale defect clusters in metallic glasses



2007 J. Phys.: Condens. Matter 19 376217

(http://iopscience.iop.org/0953-8984/19/37/376217)

IOP PUBLISHING JOURNAL OF PHYSICS: CONDENSED MATTER

J. Phys.: Condens. Matter **19** (2007) 376217 (8pp) doi:10.1088/0953-8984/19/37/376217

# Nanoscale defect clusters in metallic glasses

**P Zetterström[1,9], R Delaplane[2,9], Y D Wang[3,4], P K Liaw[4], H Choo[4], K Saksl[5], H F Zhang[6], Y Ren[7] and L Zuo[8]**

[1] Instituto de Quimica Fisica 'Rocasolano', CSIC E-28006 Madrid, Spain
[2] Borgdalsgången 36, S-611 57 Nyköping, Sweden
[3] School of Materials and Metallurgy, Northeastern University, Shenyang 110004, People's Republic of China
[4] Department of Materials Science and Engineering, The University of Tennessee, Knoxville, TN 37996, USA
[5] Deutsches Elektronen Synchrotron (HASYLAB), 22607 Hamburg, Germany
[6] Shenyang National Laboratory for Materials Science, Institute of Metal Research, Chinese Academy of Sciences, Shenyang 110015, People's Republic of China
[7] X-ray Science Division, Advanced Photon Source, Argonne National Laboratory, Argonne, IL 60439, USA
[8] Key Laboratory for Anisotropy Design and Texture Engineering of Materials (Ministry of Education), Northeastern University, Shenyang 110004, People's Republic of China

Received 3 July 2007, in final form 24 July 2007
Published 22 August 2007
Online at stacks.iop.org/JPhysCM/19/376217

**Abstract**

The reverse Monte Carlo method was used to obtain three-dimensional discrete distributions of constitutional atoms in melt-spun CuZr and CuZrTi metallic glasses from neutron and x-ray diffraction data. It was found that the icosahedral short-range order is less stable in the CuZr binary alloy than in the Ti-doped ternary alloy. The present investigation also provides evidence on the medium-range order, characterized by some nanoscale clusters of defects, in the metallic-glassy state.

## 1. Introduction

Metallic glasses have received renewed interest over the past decade due to the discovery of extraordinary glass-forming abilities in some alloy systems [1–5] giving rise to some promising structural and functional applications. It is well known that, similar to other amorphous materials, metallic glasses lack long-range translational periodicity. The nature of short- and medium-range structures in metallic glasses is much less understood than that of the well-defined crystalline structures. The complexity in determining the fine local structures in metallic glasses lies in the intrinsic metallic bonds, leading to much more flexible distributions of bonding angles and lengths as compared to those in molecular glasses. The icosahedral short-range order (ISRO), first postulated by Frank [6], has already been predicted by molecular-dynamics simulations for supercooled liquids [7–9] and then verified by numerous x-ray and

[9] Work performed at the now closed Studsvik Neutron Research Laboratory, Uppsala University, Sweden.

neutron scattering experiments on some metallic liquids [10, 11] and glasses [12–14]. However, the detailed picture on the ISRO is still lacking and cannot be visualized just from the partial distribution function (PDF) constructed with x-ray or neutron scattering data. Reverse Monte Carlo (RMC) modeling [15–17] is now a well-established method for modeling the structure of glasses and other disordered systems, showing particular advantages in the study of the medium-range order structures in metallic glasses, which has not been well investigated so far. A straightforward but naive description of the method is that Monte Carlo simulations are performed on a large number of atoms placed in a box; this configuration of atoms is then modified to best match experimental data. The structural models obtained are statistically consistent with the experiments. This method was earlier employed to generate the atomic configurations, starting from a random atomic initial configuration of Ni–Ag amorphous alloy by using EXAFS data [12, 18]. From these simulations it was concluded that there does exist a dominating ISRO, but the results still lack information on the medium-range order.

## 2. Experiments

We have made measurements for two melt-spun alloys, one binary $Cu_{50}Zr_{50}$ and one ternary $Cu_{60}Zr_{30}Ti_{10}$. Both represent typical metallic-glass systems and there have been extensive studies of the structures and various properties in the past few years [19]. It is of course not possible to separate all partial functions with only two measurements (neutron and x-ray) which is why we concentrate on Cu and Zr partials which give the strongest contribution to the total scattering. Melt-spun ribbons with a cross section of $0.03 \times 1$ mm$^2$ were prepared from ingots fabricated by arc-melting high-purity metals (99.9 at.% Zr, 99.99 at.% Cu, and 99.9 at.% Ti). The amorphous ribbons were obtained from these alloys by single-roller melt spinning at a wheel surface velocity of 30–60 m s$^{-1}$ in a purified Ar atmosphere.

Neutron scattering experiments were performed on the disordered materials diffractometer at Studsvik Neutron Research Laboratory (Sweden). The neutron wavelength used in the experiments was 1.116 Å and the diffraction patterns were collected in a $Q$ range of 0.3–10.5 Å$^{-1}$ which is sufficient for our needs. High-energy x-ray diffraction (XRD) measurements were performed at Hamburger Synchrotronstrahlungslabor (HASYLAB) at Deutsches Elektronen-Synchrotron (Germany) on the experimental station Petra2 and at the Advanced Photon Source (APS) at Argonne National Laboratory (USA) on the ID-11-C beam line using the monochromatic synchrotron radiation of 115 keV. The result was integrated to $Q$-space by using the program Fit2D [20] and the total structural factors $S(Q)$ were obtained by using the Faber–Ziman equation [21]. The structure factors for the two melt-spun alloys measured at room temperature with neutron scattering and x-ray scattering are displayed in figure 1. It is clear that the first diffraction peak of the ternary alloy is shifted to higher $Q$-values, indicating a slightly higher atomic density.

## 3. RMC simulations

Although the structural model produced by the RMC method in practice depends on the initial configuration of atomic arrangements, this method may provide an easy way to get rich structural information through the combination of neutron and x-ray scattering data. Here, our strategy has been to start from an existing icosahedral model and utilize the RMC method to modify and test the model. In this way, the RMC simulations will lower the high ISRO defined by the starting model until a good fit to experimental data is reached. The opposite approach, starting from a low ISRO (or random structure) and letting the simulation increase the order,

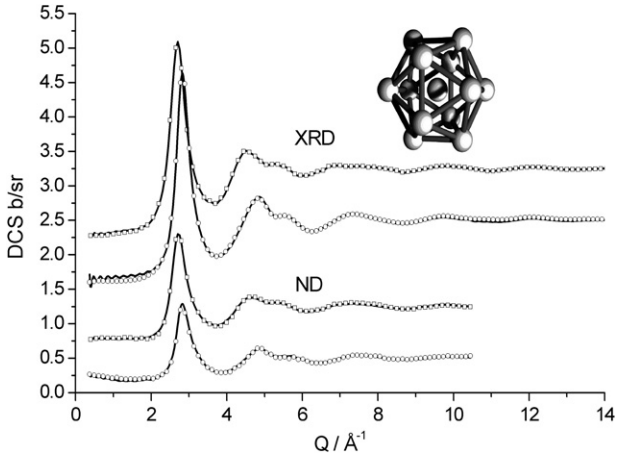


**Figure 1.** Top two and bottom two curves show measured x-ray structure factors for $Cu_{50}Zr_{50}$ (squares) and $Cu_{60}Zr_{30}Ti_{10}$ (circles). The bottom two curves show measured neutron structure factors for $Cu_{50}Zr_{50}$ (squares) and $Cu_{60}Zr_{30}Ti_{10}$ (circles). Lines are the corresponding fitted structure factors obtained with RMC. The inset figure shows 12 icosahedrally arranged atoms surrounding a central atom.

was also tested, but due to the complex landscape in the space of incommensurate curvature in the glassy state [7] this proved very difficult. The first kind of start model tried consisted of 10 000 atoms placed randomly except for an atomic separation of 2.8 Å. Good fits to measured data were obtained starting from these configurations, but as described below no clear picture of the local structure could be derived.

The second kind of start model consisted of 600 randomly placed (not overlapping) and oriented icosahedra (as shown in the top right inset of figure 1). The distances between two neighboring atoms on the icosahedra surface [13] were set to 2.7 Å. The surrounding space was filled with atoms so that the total number of atoms was 10 000. The number density used in the present simulations were 0.05 Å$^{-3}$, in agreement with the experimental density of the alloy system studied. It is worth noting that even these very crude start models reproduce many of the features seen in measured structure factors even before any fit to the data was made. During the first part of the simulation no preferred occupations were assigned for the actual atom types, Cu, Zr, or Ti. To apply coordination constraints on the configuration, each atom was marked according to its site:

(i) the central atom in an icosahedron ‘C’;
(ii) atoms on the surface of an icosahedron ‘S’; and
(iii) randomly placed atoms between icosahedra ‘R’.

Coordination constraints were set to 12 for the C–S pairs (for a pair separation between 2.47 and 2.67 Å) and 5 for the S–S pairs (pair separation between 2.6 and 2.8 Å).

Without strong constraints, the icosahedra would be destroyed at an early stage of the simulation and would give a result similar to that from a random initial configuration. At a later stage, the coordination constraints defining the icosahedral structure were relaxed. Finally the sites of real atom types were considered and new closest distances between atom types were used. We also allowed atoms of different types to swap positions. This procedure was applied to three different start configurations all giving the conclusions described below.

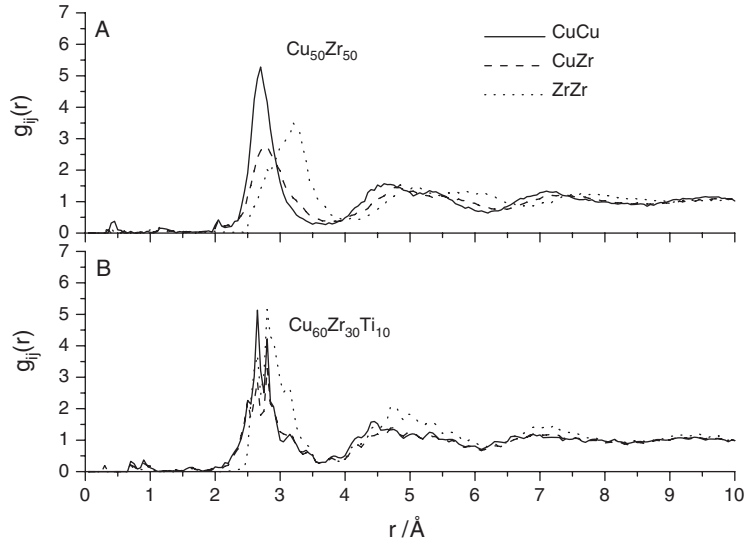


**Figure 2.** Partial $g(r)$ functions calculated from our RMC models for $Cu_{50}Zr_{50}$ (A) and $Cu_{60}Zr_{30}Ti_{10}$ (B): Cu–Cu (solid line), Cu–Zr (dashed line), and Zr–Zr (dashed–dotted line).

## 4. Results and discussion

The calculated x-ray and neutron structure factors for the melt-spun alloys are also displayed in figure 1, and are in a good agreement with experiments. Their PDFs obtained from a typical configuration are displayed in figure 2, showing that the distributions of various atomic pairs are different and that a medium-range order up to ∼1 nm exists. It can be seen from the PDFs for both $Cu_{50}Zr_{50}$ (top) and $Cu_{60}Zr_{30}Ti_{10}$ (bottom) that a relatively broad distribution exists for Zr–Zr pairs from both their first and second peaks. Another interesting observation is that the first and the second peaks in the PDFs for Cu–Cu pairs are close to those for Cu–Zr pairs, but far from the Zr–Zr pairs in both alloys. This observation is in agreement with the XRD data obtained earlier for the $Cu_{60}Zr_{30}Ti_{10}$ alloy [19].

In figures 3(A) and (B) the distributions of first-neighbour numbers around each atom at a distance less than 2.8 Å are presented. This distance has been published elsewhere [13] and gives the best indication of ISRO in our model. The fact that the first peaks in our PDFs extend above 2.8 Å is due to atoms located between icosahedral units. For an icosahedron, each central atom will be surrounded by 12 surface atoms and each surface atom will have 5 neighbouring atoms on the surface (see the inset picture in figure 1). These icosahedral-feature-like peaks are present in figure 3 although the distributions are smoothed by the distortions of icosahedra and introduction of atoms between icosahedra. It is interesting to see that the 5-neighbour peak has been shifted to a maximum value at around 3 and the 12-neighbour peak completely disappears for $Cu_{50}Zr_{50}$. However for $Cu_{60}Zr_{30}Ti_{10}$ we still find a 5-neighbour peak and a small 12-neighbour peak (which occurs in the ideal case). This trend provides evidence on the weakening of ISRO in the binary alloy. Even for the ternary alloy, we may also find that many of the original 600 icosahedra have been broken and distorted, indicating the imperfect packing of the ISRO.

Figure 4 displays the triplet distributions calculated from our models. Three atoms are considered a triplet, when the distance between members of each pair is less that 2.8 Å. We observe that triplets containing Cu, like Cu–Cu–Cu, Cu–Zr–Cu and Cu–Zr–Zr, do indeed have

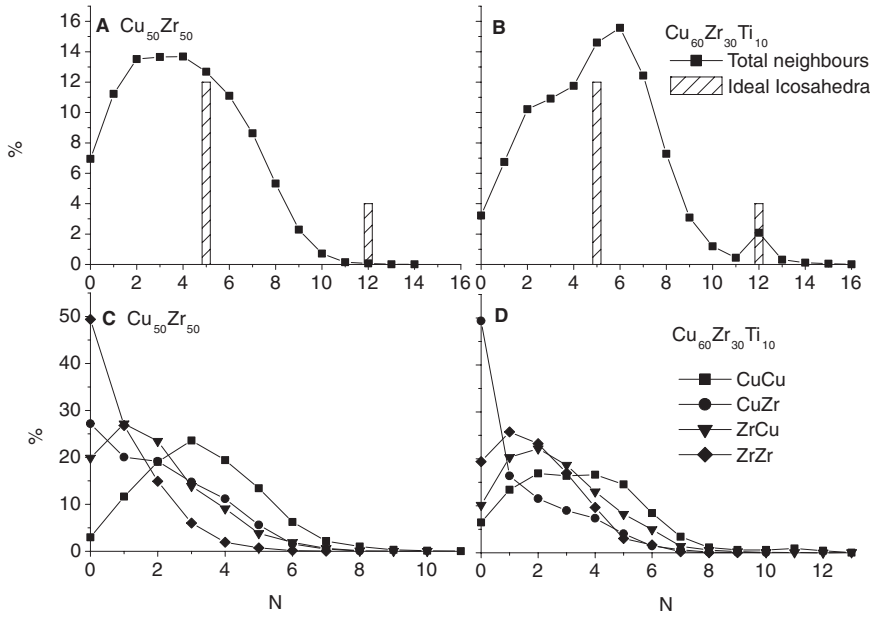


**Figure 3.** Distributions of the total first-neighbour numbers for (A) $Cu_{50}Zr_{50}$ and (B) $Cu_{60}Zr_{30}Ti_{10}$ (all neighbours are calculated for $r < 2.8$ Å). Bars indicating neighbours for an ideal icosahedron are also inserted. In (C) and (D) the distributions of neighbours for some individual atom–atom pairs are plotted.

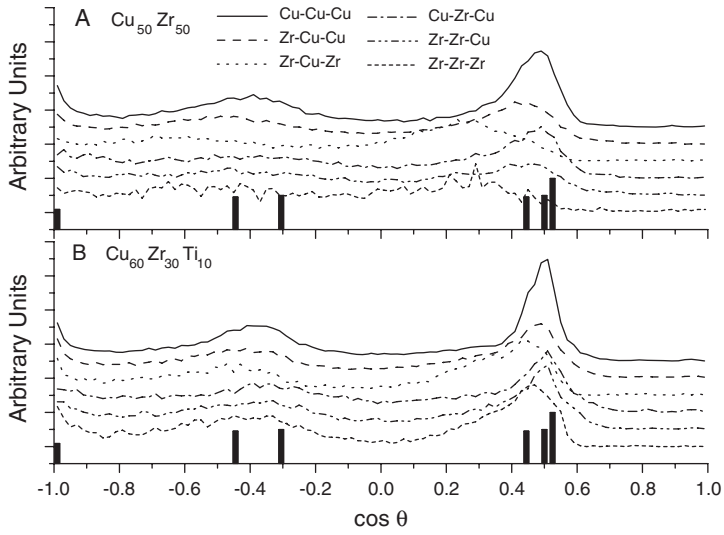


**Figure 4.** The triplet cosine distributions for (A) $Cu_{50}Zr_{50}$ and (B) $Cu_{60}Zr_{30}Ti_{10}$. The bars at the bottom of each graph show the distribution in a perfect icosahedron.

a tendency to keep the icosahedral unit, whereas the addition of the Zr element tends to weaken the ISRO. It is also evident that the Ti-doped alloy has stronger ISRO than the binary $Cu_{50}Zr_{50}$.

Figures 5(A) and (B) display the atoms in a typical configuration classified as icosahedral (C sites coordinated by 12 S sites) in the melt-spun $Cu_{50}Zr_{50}$ and $Cu_{60}Zr_{30}Ti_{10}$, respectively.

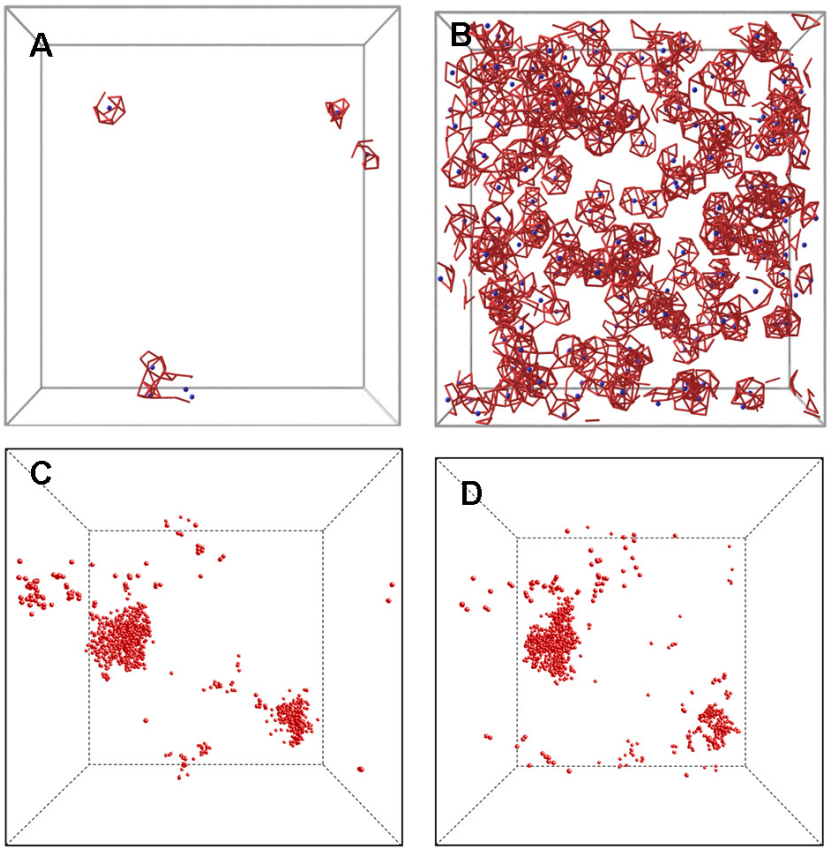


**Figure 5.** Atomic configurations for melt-spun alloys generated by reverse Monte Carlo modeling: (A) $Cu_{50}Zr_{50}$ and (B) $Cu_{60}Zr_{30}Ti_{10}$ show only the atoms which form the icosahedral arrangement. (C) $Cu_{50}Zr_{50}$ and (D) $Cu_{60}Zr_{30}Ti_{10}$ show regions of low density, points mark positions surrounded by at least 3 Å of empty space.

(This figure is in colour only in the electronic version)

In $Cu_{60}Zr_{30}Ti_{10}$ we observe clustered ISRO units of medium-range order (up to 1 nm). For the binary $Cu_{50}Zr_{50}$ alloy, this ISRO is clearly reduced.

To further investigate our models, we also used the method of Blaisten-Barojas [22, 23] to classify pairs of atoms belonging to different types of local structure. Three classes of pairs (13-atom icosahedral, FCC and HCP structure) were picked out of all those calculated. Two different cut-off distances were used. The first distance, 3.5 Å, covers the main peak in the PDF; the second distance, 2.8 Å, is the same as described above. The strongest indicators of ISRO are the 1321, 1551 and 2331 pairs. The results are given in table 1. Starting from random configurations the ISRO increased for both samples during the simulation using a cut-off distance of 3.5 Å but no other conclusions could be drawn from these calculations. Starting from the icosahedral model the ISRO is reduced for both samples during the simulations. The abundance of icosahedral structure seen as 1321, 1551 and 2331 pairs is greater for $Cu_{60}Zr_{30}Ti_{10}$ than for $Cu_{50}Zr_{50}$. Other pairs are much more influenced by FCC and HCP structures, and do not show this clear tendency. Because the start configuration influences the final result, it is not possible to prove the existence of ISRO in $Cu_{60}Zr_{30}Ti_{10}$; however the

**Table 1.** Abundance (as a percentage) for some important pairs as defined by Blaisten-Barojas. The pair calculations are for two cut-off values, 2.8 and 3.5 Å. RAN: random start configuration; ICO: icosahedral start configuration. We also mark each pairs with the type of structure it is present in (ico, fcc and hcp).

| | Cut-off: 2.8 Å | | | | Cut-off: 3.5 Å | | | |
|---|---|---|---|---|---|---|---|---|
| | $Cu_{50}Zr_{50}$ | | $Cu_{60}Zr_{30}Ti_{10}$ | | $Cu_{50}Zr_{50}$ | | $Cu_{60}Zr_{30}Ti_{10}$ | |
| Pairs | RAN | ICO | RAN | ICO | RAN | ICO | RAN | ICO |
| $1321^{ico}$ | 0.04 | 0.84 | 0 | 2.33 | 1.70 | 1.90 | 1.78 | 2.05 |
| $1551^{ico}$ | 0 | 0.06 | 0 | 0.32 | 0.92 | 1.37 | 0.74 | 1.46 |
| $2101^{hcp,fcc,ico}$ | 22.09 | 22.26 | 24.98 | 22.8 | 27.84 | 26.04 | 24.90 | 22.88 |
| $2331^{ico,hcp}$ | 0.02 | 0.71 | 0 | 2.36 | 5.74 | 7.30 | 4.96 | 7.18 |

possible ISRO in this alloy should be investigated in more detail. For $Cu_{50}Zr_{50}$ we have shown that the ISRO is not in agreement with our measured data.

To illustrate the medium-range structure we have searched for positions in our calculated structures surrounded by at least 3 Å of empty space (this distance equals that of defects in metallic glasses) and plotted them in figure 5. It can be seen from the distributions of defects that some clusters of defects with the size of about 1.3 nm do indeed exist in the metallic-glassy state. The present modeling presents evidence of clustered defects on the atomic scale in the metallic-glassy state, which goes beyond the structural topology defined by the standard method for describing covalently bonded solids [24, 25]. So far, it remains unclear whether the distributions of defects found by our modeling are intrinsically related to the well-known free volume concept widely used in bulk metallic glasses according to phenomenological theory [26]. However, from our findings, it may be predicted that internal stress fluctuations are possible on the scale of 1–2 nm in metallic glasses. Actually, the medium-range order found in the form of the nanoscale clusters of defects should be closely related to the physical and mechanical properties in Zr-based metallic glasses.

## Acknowledgments

We would like to thank P Jóvári for experimental help, and J Morris, C Fan and G Fan for valuable discussions. The present work was supported by the Swedish Research Council in the framework of the Swedish International Development Cooperation Agency (SIDA) project (Grant No. 348-2004-3475), the Ministry of Education of China (with the NCET-04-0282), the National Natural Science Foundation of China (Grant Nos 50471026, 50325102 and 50471077), and the National Science Foundation International Materials Institutes (IMI) Program with Dr C Huber as the Program Director. Use of the Advanced Photon Source was supported by the US Department of Energy, Office of Science, Office of Basic Energy Science, under Contract No. W-31-109-ENG-38.

## References

[1] Greer A L 1995 Metallic glasses *Science* **267** 1947
[2] Johnson W L 2002 Bulk amorphous metal—an emerging engineering material *J. Minerals Met. Mat. Soc.* **54** 40
[3] Inoue A 2000 Stabilization of metallic super cooled liquid and bulk amorphous alloys *Acta Mater.* **48** 279
[4] Lu Z P, Liu C T, Thompson J R and Porter W D 2004 Structural amorphous steels *Phys. Rev. Lett.* **92** 245503

[5] Xu D, Duan G and Johnson W L 2004 Unusual glass-forming ability of bulk amorphous alloys based on ordinary metal copper *Phys. Rev. Lett.* **92** 245504
[6] Frank F C 1952 A discussion on theory of liquids: supercooling of liquids *Proc. R. Soc.* A **215** 43
[7] Nelson D R 1983 Liquids and glasses in spaces of incommensurate curvature *Phys. Rev. Lett.* **50** 82
[8] Jonsson H and Andersen H 1988 Icosahedral ordering in the Lennard-Jones liquid and glass *Phys. Rev. Lett.* **60** 2295
[9] Nelson D R 2002 *Defects and Geometry in Condensed Matter Physics* (Cambridge: Press Syndicate of the University of Cambridge)
[10] Schenk T, Holland-Moritz D, Simonet V, Bellissent R and Herlach D M 2002 Icosahedral short-range order in deeply undercooled metallic melts *Phys. Rev. Lett.* **89** 75507
[11] Kelton K F, Lee G W, Gangopadhyay A K, Hyers R W, Rathz T J, Rogers J R, Robinson M B and Robinson D S 2003 First x-ray scattering studies on electrostatically levitated metallic liquids *Phys. Rev. Lett.* **90** 195504
[12] Luo W K, Sheng H W, Alamgir F M, Bai J M, He J H and Ma E 2004 Icosahedral short-range order in amorphous alloys *Phys. Rev. Lett.* **92** 145502
[13] Saksl K, Franz H, Jóvári P, Klementiev K, Welter E and Ehnes A 2003 Evidence of icosahedral short-range order in $Zr_{70}Cu_{30}$ and $Zr_{70}Cu_{29}Pd_1$ metallic glasses *Appl. Phys. Lett.* **83** 3924
[14] Sheng H W, Luo W K, Alamgir F M, Bai J M and Ma E 2006 Atomic packing and short-to-medium-range order in metallic glasses *Nature* **439** 419
[15] McGreevy R L and Pusztai L 1988 Reverse Monte Carlo simulation: a new technique for the determination of disordered structures *Mol. Simul.* **1** 359
[16] McGreevy R L 2001 Reverse Monte Carlo modelling *J. Phys.: Condens. Matter* **13** R877–913
[17] Evrard G and Pusztai L 2005 Reverse Monte Carlo modelling of the structure of disordered materials with RMC++: a new implementation of the algorithm in C++ *J. Phys.: Condens. Matter* **17** S1–13
[18] Yang L, Jiang J Z, Liu T, Hu T D and Uruga T 2005 Atomic structure in $Zr_{70}Cu_{29}Pd_1$ metallic glass *Appl. Phys. Lett.* **87** 61918
[19] Kasai M, Saida J, Matsushita M, Osuna T, Matsubara T E and Inoue A 2002 Structure and crystallization of rapidly quenched Cu–(Zr or Hf)–Ti alloys containing nano crystalline particles *J. Phys.: Condens. Matter* **14** 13867
[20] Hammersley A P, Svensson S O, Hanfland M, Fitch A N and Hausermann D 1996 Two-dimensional detector software: from real detector to idealised image or two-theta scan *High Pressure Res.* **14** 235
[21] Faber T E and Ziman J M 1965 A theory of the electrical properties of liquid metals. III. The resistivity of binary alloys *Phil. Mag.* **11** 153
[22] Blaisten-Barojas E 1984 Structural effects of three-body interactions on atomic clusters *KINAM* **6A** 71
[23] Honeycutt J D and Andersen H C 1987 Molecular dynamics study of melting and freezing of small Lennard-Jones clusters *J. Phys. Chem.* **91** 4950
[24] Zallen R 1983 *The Physics of Amorphous Solids* (New York: Wiley)
[25] Salmon P S, Martin R A, Mason P E and Cuello G J 2005 Topological versus chemical ordering in network glasses at intermediate and extended length scales *Nature* **435** 75
[26] Cohen M H and Turnbull D 1959 Molecular transport in liquids and glasses *J. Chem. Phys.* **31** 1164